

X-ray Photoelectron Study of the $\text{MoCl}_2\text{C}_{30}\text{H}_{30}$ Composite

E. G. Il'in^a, A. S. Parshakov^a, A. Yu. Teterin^b, K. I. Maslakov^b, and Yu. A. Teterin^b

^a Kurnakov Institute of General and Inorganic Chemistry, Russian Academy of Sciences,
Leninskii pr. 31, Moscow, 119991 Russia

^b Russian Research Centre Kurchatov Institute, pl. Kurchatova 1, Moscow, 123182 Russia

Received May 26, 2010

Abstract—The surface of a $\text{MoCl}_2\text{C}_{30}\text{H}_{30}$ composite in the form of molybdenum nanoclusters in a polyacetylene matrix, produced by reacting MoCl_5 with C_2H_2 in benzene and toluene, has been studied by X-ray photoelectron spectroscopy before and after Ar^+ ion milling. The composite actively reacts with atmospheric oxygen and moisture. As a result, the molybdenum clusters on its surface oxidize to molybdenum(V) or molybdenum(VI) oxides or oxychlorides ($E_b(\text{Mo } 3d_{5/2}) = 232.3\text{--}232.5 \text{ eV}$) during the sample preparation process. The electron binding energy of molybdenum after surface etching ($E_b(\text{Mo } 3d_{5/2}) = 228.5 \text{ eV}$) suggests that the oxidation state of the molybdenum in the composite is 2+ or 3+. Analysis of the structure of the spectrum of the C 2s electrons of the inner valence molecular orbitals using the energy level diagram of the C_2 molecule suggests that the hydrocarbon matrix of the composite contains, in addition to $-\text{CH}=\text{CH}-$ $\text{CH}=\text{CH}-$ conjugate bonds, linear carbyne fragments: $-\text{HC}=\text{C}=\text{CH}-$ or $-\text{C}\equiv\text{C}-$. After etching, the surface layer of the composite contained argon, which might be due to adsorption because of the small particle size of the composite or chemisorption on the surface of the polyacetylene matrix. The composite is stable in a high vacuum of $1.3 \times 10^{-5} \text{ Pa}$ up to 350°C and does not experience charging when exposed to X-rays, which indicates that it has weak dielectric properties.

DOI: 10.1134/S0020168511040145

INTRODUCTION

In X-ray photoelectron spectroscopy (XPS), information about a substance can be derived from the structure of the core-level spectra of its constituent elements [1] and the spectra of electrons in the inner and outer valence molecular orbitals (VMOs) [2]. Attention is then paid not only to chemical shifts and peak heights but also to fine-structure characteristics.

In this study, XPS is used to study the organo-inorganic composite $\text{MoCl}_2\text{C}_{30}\text{H}_{30}$, a product of the reaction between MoCl_5 and C_2H_2 , having the form of metalorganic molybdenum nanoclusters capable of catalyzing linear acetylene oligomerization in a polyacetylene matrix [3].

The objective of this work was to identify the oxidation state of the central ion in the catalytically active complex and to determine the relative concentrations of elements on the surface of the material.

EXPERIMENTAL

The starting chemicals used were MoCl_5 solutions in benzene and toluene, through which dry purified acetylene was bubbled. During the acetylene bubbling, the solution was slightly heated and changed color from dark greenish brown to black. The reaction was accompanied by HCl evolution. After the HCl release stopped, the gas was bubbled for an additional 2–3 h.

The resultant black gel-like precipitate was filtered off in an inert atmosphere, washed with a dry solvent, and dried in vacuum. After the filtration, the solution had the form of a pure solvent; that is, the forming molybdenum compounds and the acetylene oligomerization products were completely coprecipitated. The substances thus prepared had the form of fine powders unstable in air or black films insoluble in water and non-polar organic solvents but partially soluble in dimethylsulfoxide and CHCl_3 on heating. The composition of the products slightly depended on the reaction conditions (Table 1), but the Cl : Mo atomic ratio was always close to 2, and the H : C ratio was close to unity. The

Table 1. Chemical analysis of $\text{MoCl}_2\text{C}_{30}\text{H}_{30}$

Solvent	Atomic percent				Formula
	C	H	Cl	Mo	
Benzene	65.94	5.38	11.70	16.98	$\text{MoCl}_{1.86}\text{C}_{31.02}\text{H}_{30.10}$
Toluene	66.23	5.24	11.87	16.66	$\text{MoCl}_{1.93}\text{C}_{31.75}\text{H}_{29.88}$

Table 2. Binding energies (E_b) and full width at half maximum (Γ) of lines for MoCl₂C₃₀H₃₀ samples

Sample no.	Synthesis conditions	E_b , eV (Γ , eV)				
		Outer VMOs	Mo 3d _{5/2}	Cl 2p _{3/2}	O 1s	C 1s*
1	Synthesis in benzene	5.5(3.0)	232.4 (1.6)	198.1	532.0 (3.1)	284.0
		12.2		199.7 (1.5)		285.4
		17.9				286.5
		24.8				288.0 (1.3)
2	Synthesis in toluene (assay 1)	5.5 (2.8)	232.3 (2.0)	198.2	531.4	284.0
		12.3		199.7 (1.5)	532.7	285.4
		18.1			534.5 (2.1)	286.4
		—				287.7 (1.3)
3	Synthesis in toluene (assay 1), etching with Ar ⁺ for 5 min	16.4 (~10)	228.5 (1.3)	198.0 199.5 (1.6)	532.0 (2.7)	284.0 (1.3)
4	Synthesis in toluene (assay 2)	6.1 (3.4)	232.5 (1.9)	198.1	532.0 (3.1)	284.0
		12.2		199.6 (1.6)		285.3
		17.9				286.4
5	Synthesis in toluene (assay 2), etching with Ar ⁺ for 1 min	12.7	228.5	198.0	531.9 (2.4)	284.0 (1.3)
		17.7	232.4 (1.4)	199.5 (1.5)		
6	Mo foil	1.7 (4.3)	227.8 (1.2)			
	MoO ₂ on Mo		229.4 (1.2)			
7	Mo [4]		228.0			
8	MoO ₂ [1]		229.9		531.3	
9	MoO ₃ [1]		233.2		531.8	
10	MoOCl ₃ (Ph ₃ P) ₂ [1]		232.5	198.3		

* 284.0 eV is referred to graphite.

substances were stable in an inert atmosphere and high vacuum (1.3×10^{-5} Pa) up to 350°C.

XPS spectra of MoCl₂C₃₀H₃₀ were measured on a VG Scientific ESCALAB MK II electrostatic spectrometer at room temperature in a vacuum of 1.3×10^{-7} Pa using radiation from an Al $K_{\alpha 1,2}$ X-ray source (1486.6 eV). The spectrometer resolution was 1.2 eV. As the binding-energy-scale reference, we used the C 1s level (285.0 eV) arising from hydrocarbons on a Au plate (Table 2). The uncertainties in the binding energies E_b and peak widths Γ obtained were 0.1 eV. Relative intensities were measured to an accuracy of 10%. The FWHM was determined relative to that of the C 1s peak of hydrocarbons on gold: $\Gamma(\text{C } 1\text{s}) = 1.3$ eV.

Fine-particle samples (sample 1, synthesized in benzene, and samples 2–5, synthesized in toluene (Table 1)) were applied in the form of thick layers to a conductive two-side adhesive tape (samples 2–5) or pressed into indium on a titanium substrate (sample 1).

The sample surface was Ar⁺-ion-milled at a gun current of 5 μA ($j = 1 \mu\text{A}/\text{cm}^2$) and voltage of 3 kV. The surface of Mo foil (sample 6) was cleaned mechanically,

and then we measured its XPS spectrum, etched the foil, and again measured its spectrum.

The binding energy scale was calibrated for each individual peak. To this end, the C 1s spectrum was recorded before and after obtaining each peak, which reduced the uncertainty in binding energies to 0.1 eV.

In quantitative elemental and ionic analyses, we used the relation

$$n_i/n_j = (S_i/S_j)(k_j/k_i),$$

where n_i/n_j is the relative concentration of the atoms of interest, S_i/S_j is the relative intensity of the core-level peaks of these atoms, and k_j/k_i is the experimentally determined relative sensitivity factor (we used $k_j/k_i = 1.00$ (C 1s), 2.64 (O 1s), 0.10 (O 2s), 2.92 (Cl 2p), and 11.00 (Mo 3d) [4]).

RESULTS AND DISCUSSION

Survey spectra (0–1250 eV) of the composite showed lines of its constituent elements and oxygen (Table 1, Fig. 1).

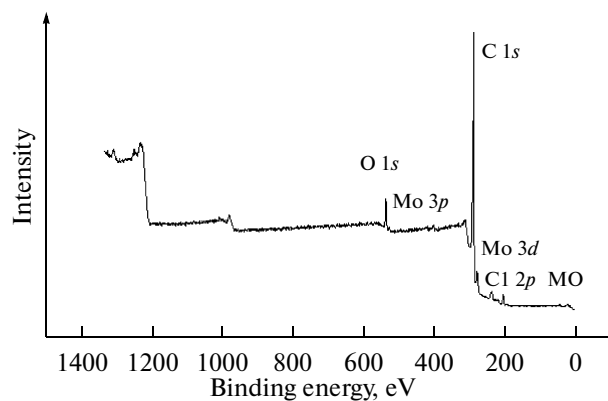


Fig. 1. Survey XPS spectrum of sample 2 of the $\text{MoCl}_2\text{C}_{30}\text{H}_{30}$ composite.

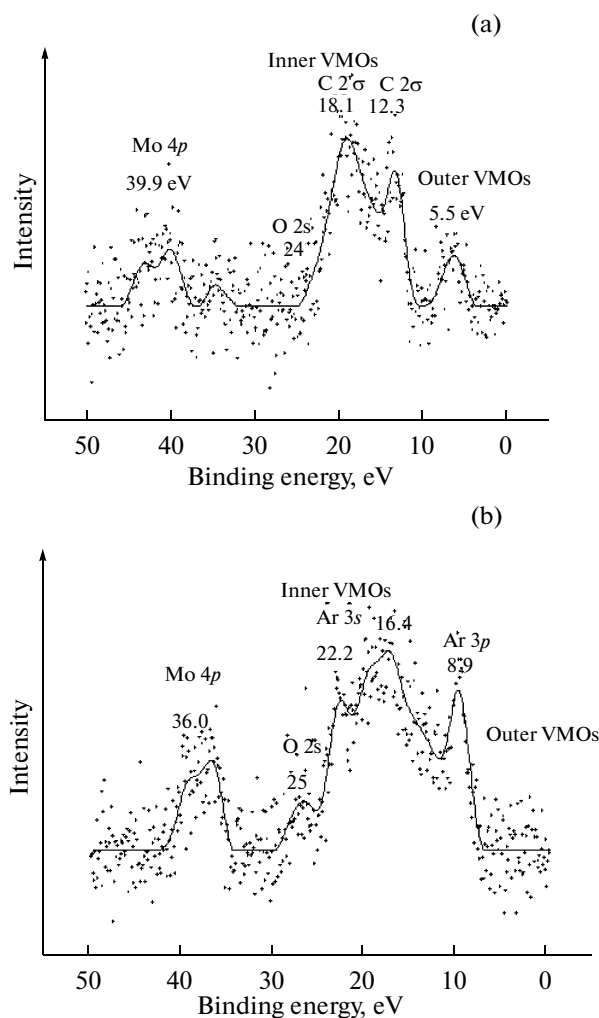


Fig. 2. XPS spectra of the $\text{MoCl}_2\text{C}_{30}\text{H}_{30}$ composite in the range 0–50 eV: (a) before Ar^+ ion milling (sample 2), (b) after milling (sample 3).

At binding energies from 0 to ~13 eV, we observed lines of outer VMOs, derived mainly from neighboring atoms. The range from ~13 to ~50 eV corresponds in larger measure to inner VMOs, and binding energies above 50 eV correspond to core levels [5].

Figure 2 shows the low-energy spectrum (0–50 eV). The 5.5-eV band corresponds to the outer VMOs derived from the Mo 5d, Mo 5s, Cl 3p, C 2p, and O 2p levels. The lines in the range 13 to 50 eV are due to the C 2s, Cl 3s, O 2s, and Mo 4p inner levels of the VMOs (Fig. 2a, Table 2).

In the spectra taken before etching (samples 1 and 2), the C 2s level of the inner VMOs was observed at ~18 (higher energy component $\text{C } 2\sigma_g$) and ~12 eV (lower energy component $\text{C } 2\sigma_u$) (samples 1 and 2). After etching (sample 3), the structure was broader, and a broad band ($\Gamma \sim 10$ eV) was present at 16.4 eV (Fig. 2b, Table 2). Also present in this region were the Ar 3s and Ar 3p lines of adsorbed atoms (Fig. 2b). Since the photo effect cross section for the C 2s level is a factor of 31.8 larger than that for the C 2p level [6], the XPS spectrum of the valence region is due to the C 2s level.

To determine the structure of the organic component of the composite, consider in greater detail the structure of the $\text{C } 2\sigma_g$ and $\text{C } 2\sigma_u^*$ lines using the energy level diagram of the C_2 molecule (Fig. 3). The valence region is due to the outer electrons of the VMOs, which have a C 2p character, and the band bottom is formed by the outer electrons of the VMOs, which predominantly have a C 2s character. An estimate by the total energy separation method [7] indicates that the contributions of the inner VMOs to the covalent bonding energy relative to the corresponding contributions of all the MOs of the C_2 molecule and C_2^- and C_2^{2-} clusters at the equilibrium bond lengths are 57, 58, and 58%, respectively. When carbon atoms approach one another, they form a system of MOs. At large bond lengths ($\Delta'_i > \Delta_i$) (see

Fig. 3), the electrons of the $\text{C } 2\sigma_u^*$ inner VMOs loosen the bond slightly more than the $\text{C } 2\sigma_g$ electrons strengthen it (Fig. 3a) [7]. As the atoms approach one another further, the $\text{C } 3\sigma_g$ outer VMOs and $\text{C } 2\sigma_g$ inner VMOs partially lose their bonding and antibonding character, whereas the bonding character of the $\text{C } 2\sigma_g$ inner VMOs becomes more pronounced (Fig. 3b). As a result, the $\text{C } 2\sigma_g$ and $\text{C } 2\sigma_u^*$ electrons of the inner VMOs may make an overall positive contribution to the bonding energy of the C_2 molecule. Indeed, calculation results (CNDO/2) indicate that, with decreasing $R_{\text{C}-\text{C}}$ bond length, the MO energies vary exactly this way (Fig. 4). An inversion of the $\text{C } 3\sigma_g$ and $\text{C } 1\pi_u$ levels of the outer VMOs occurs when $R_{\text{C}-\text{C}}$ decreases to ~0.17 nm for C_2 and to ~0.14 for the C_2^- and C_2^{2-} clusters. The energy difference $\Delta E(\text{C } 2\sigma_u^* - \text{C } 2\sigma_g)$ at the

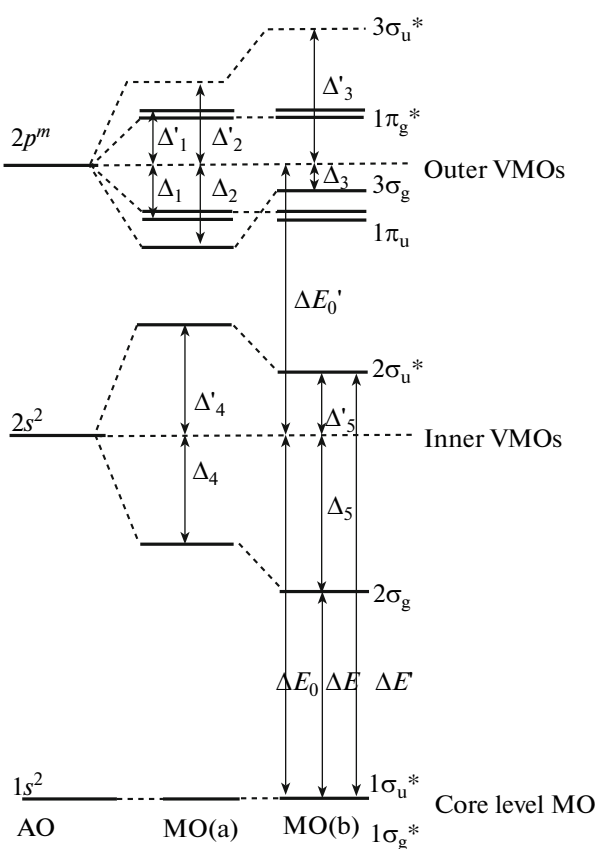


Fig. 3. Schematic illustrating the formation of the MOs of the C_2 molecule from the C 1s, C 2s, and C 2p AOs: (a) no intermixing between the outer and inner valence AOs; (b) AOs intermix (the chemical shift of the levels upon the formation of the molecule is not shown; the diagram specifies Δ_i and ΔE_i that can be measured experimentally).

bond lengths in C_2 (0.1242 nm), C_2^- (0.1263 nm), and C_2^{2-} (0.1284 nm) is 18.2, 16.8, and 15.4 eV, respectively.

These data are in qualitative agreement with more rigorous calculations of the electronic structure of graphite [8] and with data derived from orbital forces [9], but they are larger in magnitude because the CNDO/2 method is only approximate.

It is of interest to compare these results with the valence electron spectrum of carbyne (Fig. 5) [10], containing $-\text{HC}=\text{C}=\text{CH}-$ or $-\text{C}\equiv\text{C}-\text{C}\equiv\text{C}-$ linkages [11]. Indeed, the electronic spectrum of carbyne has two well-defined peaks attributable to the $\text{C}2\sigma_g$ and $\text{C}2\sigma_u^*$ electrons of the inner VMOs (Figs. 4, 5). Moreover, the considerable broadening of the $\text{C}2\sigma_g$ line of the inner VMOs in comparison with the $\text{C}2\sigma_u^*$ line confirms that the $\text{C}2\sigma_g$ electrons bond to a greater extent than the $\text{C}2\sigma_u^*$ electrons loosen (Figs. 3, 4). This fact agrees with the XPS data for the linear molecules of saturated hydrocarbons [12], but the calculated energy dif-

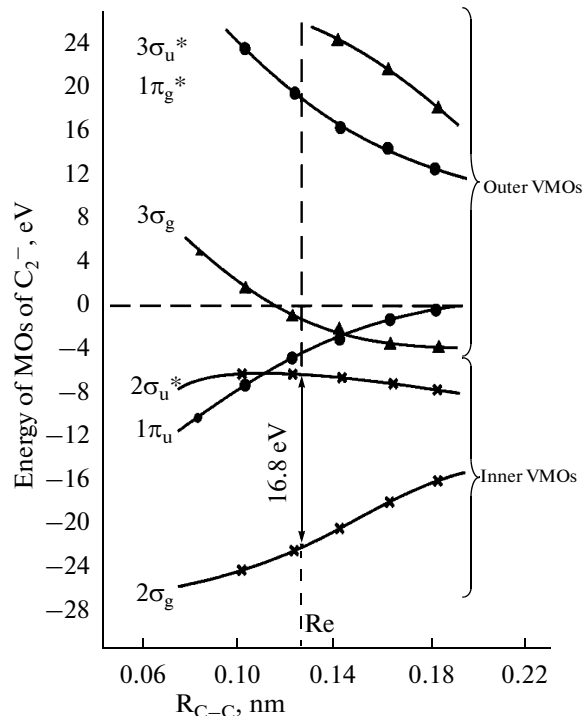


Fig. 4. Energy of the MOs of the C_2^- cluster as a function of the $R_{\text{C}-\text{C}}$ bond length (CNDO/2) [7].

ference $\Delta E(\text{C}2\sigma_u^* - \text{C}2\sigma_g) = 18.2$ eV for the C_2 molecule far exceeds the corresponding value for carbyne (Fig. 5) [10].

Even though the model under consideration is simplified, its results provide a qualitative understanding of the fine structure of the measured valence electron XPS spectrum of the composite in the carbon region (Figs. 2a, 3) and leads us to conclude that the hydrocarbon matrix contains linear carbyne linkages, $-\text{HC}=\text{C}=\text{CH}-$ or $-\text{C}\equiv\text{C}-$.

Before etching, the $\text{Mo}4p_{3/2}$ line was observed at 39.9 eV. Etching sharply reduced its intensity and gave rise to an extra line at 36.0 eV (Fig. 2, Table 2), which can be interpreted as evidence that the material contains molybdenum atoms in lower oxidation states, and correlates with the change in $\text{Mo}3d_{5/2}$ binding energy (Table 2).

The broad O 2s line (at ~ 24 eV) was weak because of the low oxygen content compared to carbon. The weak Cl 3s line should be located at 17.4 eV and may overlap with the higher energy component $\text{C}2\sigma_g$ of the outer VMOs.

The XPS spectra showed strong C 1s, O 1s, Cl 2p, and Mo 3d core level lines (Table 2), which are commonly used to assess the oxidation state of the element and to carry out quantitative elemental and ionic analyses [1, 4, 5]. The C 1s spectrum showed a strong line overlapping with a number of weaker lines on the high-energy side, which reflects the presence of chemically

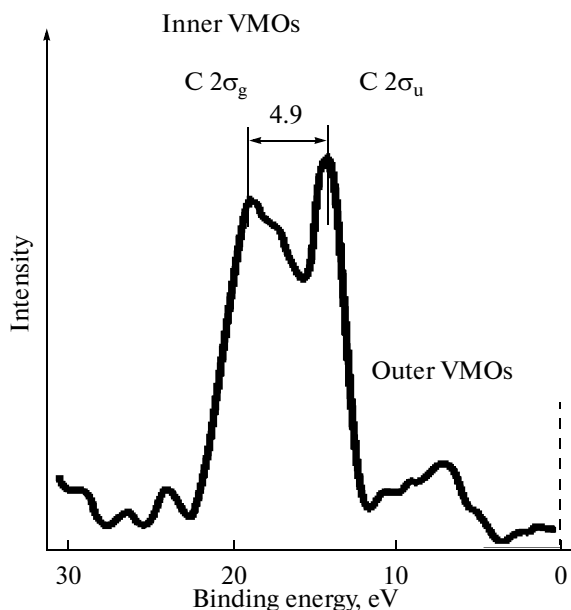


Fig. 5. Valence electron XPS spectrum of carbyne [10].

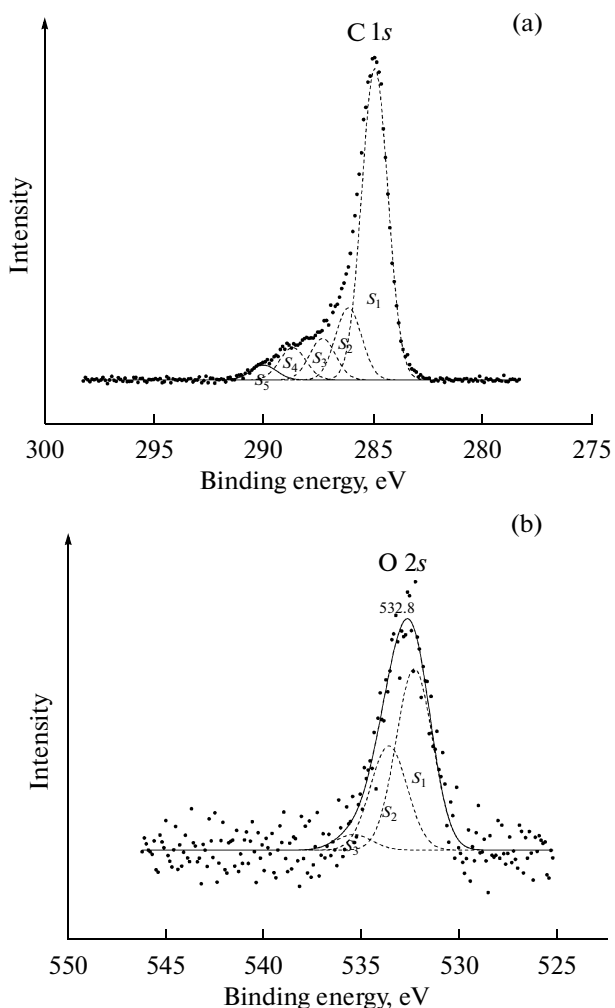


Fig. 6. XPS spectrum of sample 2: (a) C 1s region, (b) O 1s region.

inequivalent carbon atoms (Fig. 6a, Table 2). The strongest line at 284.0 eV is attributable to the CH groups of the polyacetylene matrix; the lines at 285.4 and 286.4 eV, to the carbon atoms in the terminal groups =CH₂ or =CHCl; and the states at 287.7 and 289.1 eV, to carbons coordinated to oxygens (Fig. 6a, Table 2).

The O 1s spectrum (Fig. 6b) had the form of a broadened line at ~532 eV, indicating the presence of oxygen ions in various chemical states. Because the shape of the line had no clear maxima, the uncertainty in decomposing it into components was rather high, so only the spectrum of sample 2 was decomposed (Fig. 6b; Table 2). The O 1s binding energies obtained (531.4, 532.7, and 534.5 eV) were used to estimate the bond lengths of the oxygen atoms as [13]

$$R_{M-O} (\text{nm}) = 2.27 (E_b - 519.4)^{-1}. \quad (1)$$

The R_{M-O} values obtained, 0.189, 0.171, and 0.150 nm, are likely to correspond to Mo—O—Mo, Mo=O, and C—OH bonds, respectively.

Etching markedly reduced the intensity of the O 1s line, by a factor of 3–4. The Cl 2p line—usually a poorly resolved doublet due to spin–orbit coupling with $\Delta E_{sl} = 2.0$ eV—had a more complex shape (Fig. 7), consisting of two overlapping doublets (Fig. 7) at 198.2 and 199.7 eV (sample 2, Table 2). This may be due to the presence of two inequivalent chlorine atoms bonded, e.g., to Mo atoms (by terminal and bridge bonds) or carbon atoms. These two states of chlorine atoms persisted after argon ion milling of the surface.

Before etching, the Mo 3d line in the spectrum of the composite had the form of a characteristic doublet with a spin–orbit splitting $\Delta E_{sl} = 3.0$ eV (Fig. 8a). The binding energy E_b (Mo 3d_{5/2}) = 232.5 eV (sample 4, Table 2) corresponded to molybdenum in the oxidation state 5+ (Table 2), which pointed to the oxidation of the surface of the composite by atmospheric oxygen and moisture during sample preparation. Surface etching for 1 min (sample 5) markedly reduced the intensity of this line and gave rise to a strong line at 228.5 eV, attributable to Mo (2+ or 3+) in the unoxidized composite cluster, and to a line at 241.5 eV, due to adsorbed argon (Ar 2p_{3/2}). In sample 3, the argon content on the surface of the composite exceeded the molybdenum content by a factor of 2.8. Since no argon was detected on the surface of the molybdenum platelet after etching, we believe that argon was adsorbed because of the small particle size or chemisorbed by the hydrocarbon matrix.

Etching for 5 min removed the oxidized layer, and only the 228.5-eV line was observed (sample 3, Table 2). The E_b (Mo 3d_{5/2}) is 229.9 eV in MoO₂, 233.2 eV in MoO₃, and 228.0 eV in Mo (Table 2). The E_b (Mo 3d_{5/2}) in the composite (228.5 eV) slightly exceeds that in Mo but is substantially lower than that in MoO₂. It is therefore reasonable to assume that the molybdenum in the cluster of the composite is in the oxidation states 2+ and 3+.

Quantitative elemental and ionic analyses were carried out using the intensities of the lines and the sensi-

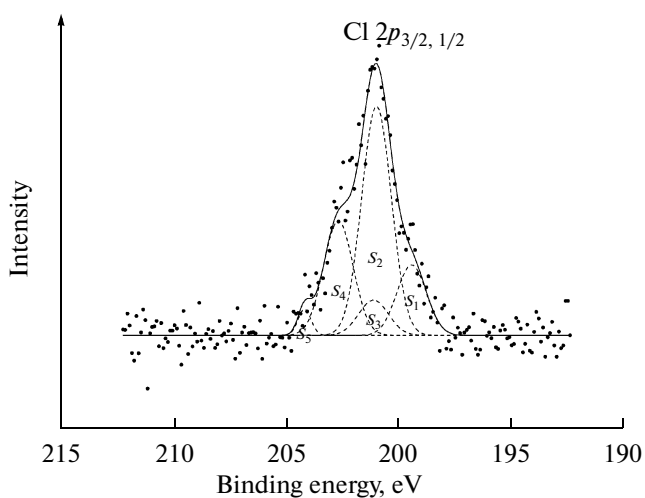
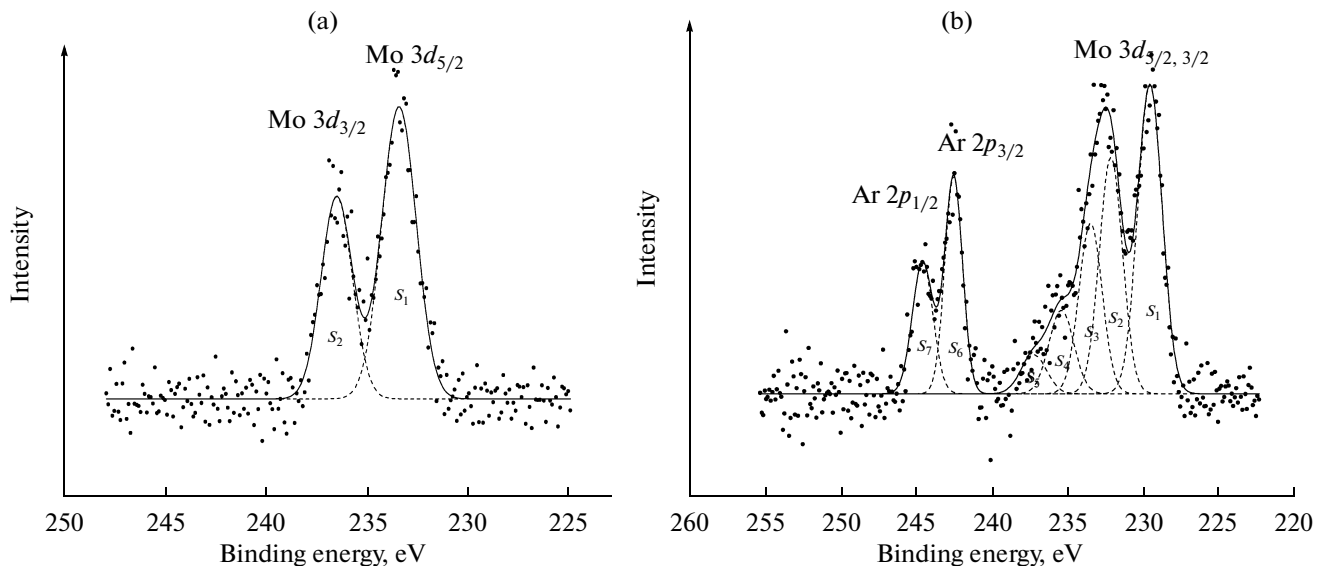
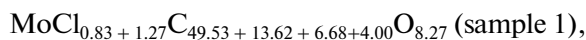


Fig. 7. XPS spectrum of sample 2 in the Cl 2p region.

Fig. 8. XPS spectra in the Mo 3d region: (a) sample 4 (assay 2), (b) sample 5 (assay 2, after Ar^+ milling).

tivity factors relative to molybdenum [4]. As a result, the following formula was obtained:



that is, there are about two chlorine atoms and more than eight oxygens per molybdenum atom on the surface of the sample. The number of carbon atoms is overestimated because carbon was present in the adhesive tape.

CONCLUSIONS

We have measured the electron binding energy of molybdenum in the nanocluster of the $\text{MoCl}_2\text{C}_{30}\text{H}_{30}$ composite: $E_b(\text{Mo } 3d_{5/2}) = 228.5$ eV. Comparison of this value with literature data leads us to assume that the oxidation state of the molybdenum in the nanocluster is

2+ or 3+, which slightly exceeds that in metallic molybdenum ($E_b(\text{Mo } 3d_{5/2}) = 227.8$ eV) and is substantially lower than that in molybdenum dioxide ($E_b(\text{Mo } 3d_{5/2}) = 229.9$ eV).

Because of its small particle size, the composite actively reacts with atmospheric oxygen and moisture. As a result, the molybdenum ions of the nanoclusters of lower chlorides oxidize to molybdenum(V) or molybdenum(VI) oxides/oxychlorides during the sample preparation process.

The study of the structure of the spectrum of the C 2s electrons of the inner VMOs of the composite and calculation of the structure of the $\text{C } 2\sigma_g$ and $\text{C } 2\sigma_u^*$ spectra using the energy level diagram of the C_2 molecule suggest that the polyacetylene hydrocarbon matrix contains linear carbyne linkages: $-\text{HC}=\text{C}=\text{CH}-$ or $-\text{C}\equiv\text{C}-$.

We detected capture and stabilization of argon ions in the surface layer of the composite, which may be due to adsorption because of the small particle size of the composite or chemisorption on the surface of the polyacetylene matrix.

The composite is stable in high vacuum and does not experience charging when exposed to X-rays, which indicates that it has weak dielectric properties.

REFERENCES

- Nefedov, V.N., *Rentgenoelektronnaya spektroskopiya khimicheskikh soedinenii* (X-ray Photoelectron Spectroscopy of Chemical Compounds), Moscow: Khimiya, 1984.
- Teterin, Yu.A. and Gagarin, S.G., Inner Valence Molecular Orbitals of Compounds and the Structure of X-Ray Photoelectron Spectra, *Usp. Khim.*, 1996, vol. 65, no. 10, pp. 895–912.
- Il'in, E.G., Parshakov, A.S., Buryak, A.K., et al., Molybdenum Chloride Nanoclusters: Active Centers in Catalytic Acetylene Oligomerization Processes, *Dokl. Akad. Nauk*, 2009, vol. 427, no. 5, pp. 641–645.
- Practical Surface Analysis by Auger and X-ray Photoelectron Spectroscopy*, Briggs, D. and Seah, M., Eds., New York: Wiley, 1983.
- Teterin, Yu.A. and Teterin, A.Yu., Structure of X-ray Photoelectron Spectra of Lanthanide Compounds, *Usp. Khim.*, 2002, vol. 71, no. 5, pp. 403–441.
- Scofield, J.H., Hartree–Slater Subshell Photoionization Crosssections at 1254 and 1487 eV, *J. Electron Spectrosc. Relat. Phenom.*, 1976, vol. 8, pp. 129–137.
- Teterin, Yu.A., Gagarin, S.G., and Baev, A.S., X-ray Photoelectron Study of Pyrolytic Graphite, in *Poverkhnostnye i teplofizicheskie svoistva almazov* (Thermophysical and Surface Properties of Diamond), Kiev: Inst. Sverkhtverdykh Materialov Akad. Nauk USSR, 1985, pp. 17–21.
- Baitinger, E.M. and Gagarin, S.G., Interatomic Interaction in Graphite, in *Fizicheskie svoistva uglerodnykh materialov* (Physical Properties of Carbon Materials), Chelyabinsk: ChPGI, 1983, pp. 82–85.
- Averill, F.W. and Painter, G.S., Orbital Forces and Chemical Bonding in Density-Functional Theory: Application to First-Row Dimers, *Phys. Rev. B: Condens. Matter Mater. Phys.*, 1986, vol. 34, no. 4, pp. 2088–2096.
- Korshak, V.V., Baitinger, E.M., Kugeev, A.S., et al., Variation in the Electronic Structure of the Chain during Carbyne Synthesis, *Dokl. Akad. Nauk SSSR*, 1988, vol. 303, no. 4, pp. 894–897.
- Sergushin, I.P., Kudryavtsev, Yu.P., Elizan, V.M., et al., X-Ray Photoelectron and X-Ray Emission Study of Carbyne, *Zh. Strukt. Khim.*, 1977, vol. 18, no. 4, pp. 698–773.
- Pireaux, J.J., Svensson, S., Basilier, E., et al., Core-Electron Relaxation Energies and Valence-Band Formation of Linear Alkaner Studied in the Gas Phase by Means of Electron Spectroscopy, *Phys. Rev. A*, 1976, vol. 14, no. 6, pp. 2133–2145.
- Sosulinikov, M.I. and Teterin, Yu.A., X-ray Photoelectron Study of Calcium, Strontium, Barium, and Their Oxides, *Dokl. Akad. Nauk SSSR*, 1991, vol. 317, no. 2, pp. 418–421.